Cretaceous Research 150 (2023) 105594

Contents lists available at ScienceDirect

Cretaceous Research

journal homepage: www.elsevier.com/locate/CretRes

Short communication

Assessing the palaeobiology of *Vespersaurus paranaensis* (Theropoda, Noasauridae), Cretaceous, Bauru Basin – Brazil, using Finite Element Analysis

Gabriel Gonzalez Barbosa [a, b, *], Max Cardoso Langer [c], Neurides de Oliveira Martins [d], Felipe Chinaglia Montefeltro [a, b]

[a] Laboratório de Paleontologia e Evolução de Ilha Solteira, UNESP, Ilha Solteira, Brazil
[b] Programa de Pós-Graduação em Biodiversidade, UNESP, São José Do Rio Preto, Brazil
[c] Laboratório de Paleontologia, Faculdade de Filosofia, Ciências e Letras de Ribeirão Preto, Universidade de São Paulo, Brazil
[d] Museu de Paleontologia de Cruzeiro Do Oeste, Cruzeiro Do Oeste, PR, Brazil

ARTICLE INFO

Article history:
Received 14 September 2022
Received in revised form
9 May 2023
Accepted in revised form 24 May 2023
Available online 26 May 2023

Keywords:
Functional morphology
Caiuá Group
Bauru Basin

ABSTRACT

Noasauridae is a group of theropod dinosaurs mostly present in Gondwanan deposits of Jurassic and Cretaceous age. *Vespersaurus paranaensis* from the Bauru Basin (Caiuá Group, Cretaceous) was the first Brazilian taxon assigned to the clade. This work applied Finite Element Analysis (FEA) to investigate the functional morphology of some skeletal elements assigned to *Ves. paranaensis* (one tooth and two pedal ungual phalanges). The tooth was modeled and tested in six different scenarios to infer the performance of its crown in different putative feeding conditions. Three different extrinsic scenarios were tested on the ungual phalanges to simulate potential habits in which these structures were involved (piercing, scratch-digging, and hook-and-pull). The scenarios tested on the tooth suggest an ideal bite angle of 45°, with higher von Mises stress/element in the other angles. This indicates that the dentition of this noasaurid was not adapted for struggling prey, nor for harder food items. The FEA results of the ungual phalanges of *Ves. paranaensis* suggest a similar performance in the three tested scenarios, therefore not specifically adapted for any of those specific functions. Additionally, these phalanges are similar in shape to those of living mammals with scansorial, fossorial, and terrestrial habits. Collectively, this information suggests that, *Ves. paranaensis* had a generalist diet, seeking to hunt small vertebrates, invertebrates, or immobile prey, such as carcass, and did not feed on larger animals.

1. Introduction

Noasauridae is a clade of theropod dinosaurs nested within Abelisauroidea. The group was originally erected (Bonaparte and Powell, 1980) to encompass only *Noasaurus leali*, from the Maastrichtian of Salta, Argentina. The description of several new species expanded the taxonomic and morphological diversity of the group, containing species described in South America, Africa, Madagascar, India, Europe and Australia (Bonaparte, 1996; Coria and Salgado, 2000; Sampson et al., 2001; Carrano et al., 2002; Agnolin and Martinelli, 2007; Carrano et al., 2011; Pol and Rauhut, 2012; Tortosa et al., 2014; Poropat et al., 2020). However, noasaurids are still mainly known by rather incomplete records from the Cretaceous of Gondwana (Brum et al., 2018; Brougham et al., 2020; de Souza et al., 2021).

The fragmentary nature of most noasaurid specimens reveals an overall picture composed of small to medium-sized dinosaurs with necks, arms, and skulls relatively longer than those of other abelisauroid clades (Xu et al., 2009; Carrano et al., 2011). However, little is known about the paleobiology of the group, including their diet, even though an apparent great internal disparity was detected, such as edentulous and toothed species, implying different feeding habits (Novas et al., 2013; Egli et al., 2016; de Souza et al., 2021). The functionality of their ungual phalanges is also not much debated, but morphologically, they resemble those of early theropods, with the prehensile function of alleged "raptorial" habits (Carrano et al.,

* Corresponding author. Laboratório de Paleontologia e Evolução de Ilha Solteira, UNESP, Ilha Solteira, Brazil.
E-mail addresses: gabriel.gonzalez@unesp.br (G.G. Barbosa), mc.langer@ffclrp.usp.br (M.C. Langer), neurides.martins@gmail.com (N. de Oliveira Martins), fc.montefeltro@unesp.br (F.C. Montefeltro).

https://doi.org/10.1016/j.cretres.2023.105594
0195-6671/

2011). Even with newly described species, a more comprehensive understanding of the evolutionary history and morphoanatomical trait distribution is still lacking for noasaurids, as well as their significance within the broader context of theropod evolution (de Souza et al., 2021).

The Caiuá Group is a geologic unit assigned to either the Early (Bruckmann et al., 2014; Batezelli & Ladeira, 2016) or Late (Fernandes & Ribeiro, 2015; Batezelli & Ladeira, 2016; Menegazzo et al., 2016; Castro et al., 2018) Cretaceous in the available stratigraphic proposals. The Rio Paraná Formation, within the Caiuá Group, was deposited under a desertic paleoenvironment, likely with water bodies lasting among the dunes. Two noasaurid theropod dinosaurs are known from this unit: *Vespersaurus paranaensis* (Langer et al., 2019) and *Berthasaura leopoldinae* (de Souza et al., 2021). *Ves. paranaensis* is a small and medium-sized noasaurid (80 cm high and 1.5 m long) and is considered one of the best preserved theropods in Brazil (de Souza et al., 2020), but little information about feeding habits of this species has been explored, as well as ungual phalanges functions, and paleobiology. Finite Element Analysis (FEA) is a powerful tool to understand and test biomechanic and functional morphology hypotheses about extinct taxa (Richmond et al., 2005; Ross, 2005; Rayfield, 2007; Tseng, 2009; Grine et al., 2010). Here, with the aim of complementing the information about the paleobiology of *Ves. paranaensis*, we inferred its feeding habits based on the performance of dental and pedal elements using FEA.

2. Materials

The materials analyzed here include an isolated tooth MPCO.V 0020c (Museu de Paleontologia de Cruzeiro do Oeste, Brazil) and ungual phalanges of a right digit IV (MPCO.V 0022) and left digit I (MPCO.V 0036a), which have been assigned to *Ves. paranaensis* by Langer et al. (2019). This species is assigned to the Rio Paraná Formation, Caiuá Group, Bauru Basin (Fernandes & Ribeiro, 2015; Langer et al., 2019).

The isolated tooth (MPCO.V 0020c; Fig. 1A–E) is composed of an almost complete crown, 5 mm apicobasally long, 4 mm mesiodistally broad, and slightly curved labiodistally (approximately 10°). Serrations are present on the mesial and distal carinae, with a density of approximately 4 denticles per millimeter (Fig. 1B–E). The distal serrations extend from the base to the apex of the crown, whereas the mesial serrations start 1 mm from the base of the crown and extend to the apex. The crown apex has signs of wear, probably due to use during the animal's life. The material was assigned to the rostral part of the tooth rows (Langer et al., 2019). The ungual phalange MPCO.V 0022 (Fig. 1F–J) is approximately 30 mm long and has a subtriangular shape; the ventral margin is straight, and the dorsal margin is slightly convex. The other ungual phalange (MPCO.V 0036a. Fig. 1K–O) is much smaller, 9 mm in total length, with a dorsoventral depth of about 6 mm (therefore, more robust than MPCO.V 0022), and convex ventral and dorsal margins. The phalanges have longitudinal grooves on both sides, representing the abelisauroid system of vascular grooves, with a "Y-shaped" distribution (Langer et al., 2019).

3. Methods

The tooth and the ungual phalanges were subject to computed tomography (CT) in the Micro-CT machine GE Phoenix v|tome|x, available at the "Centro para Documentação da Biodiversidade", Universidade de São Paulo (USP - Ribeirão Preto, Brazil). The tooth MPCO.V 0020c was scanned with voxel size of 0.135294 mm × 0.135294 mm × 0.135294 mm, 732 slices, and 150,000 faces; the phalanx of right digit IV MPCO.V 0022 was scanned with voxel size of 0.135294 mm × 0.135294 mm × 0.135294 mm, 1000 slices, and 250,000 faces; the phalanx of left digit I MPCO.V 0036a was scanned with voxel size of 0.0351338 mm × 0.0351337 mm × 0.0351339 mm, 732 slices, and 125,000 faces. The CT scans of all three elements are available upon request to the authors. The CT data was segmented in Amira 5.3.3 (Thermo Fisher Scientific) and also subject to slight restoration (filling small cracks and adjusting deformed parts) to account for taphonomic distortion and breakages.

The 3D models were imported into *Hypermesh* (v. 11, Altair Engineering) for transformation into solid tetra-mesh. All three models have 676,560 elements, with volumes of 20.339 for the tooth and 300,000 for each phalanx. The properties applied to the tooth were $E = 25$ Gpa and $\upsilon = 0.31$, whereas those of the phalanges were $E = 20.49$ Gpa and $\upsilon = 0.31$ (Lautenschlager, 2014). All materials were treated as isotropic and homogeneous. The area of the tooth model was scaled to allow proper comparison with the dental models presented by Torices et al. (2018) (Dumont et al., 2009; Bright, 2014) and the phalanx models followed the scale and properties of Lautenschlager (2014) for comparisons.

We constrained the tooth at the denticles from the distalmost part of the crown (Fig. 2A and B). We applied a total of 90 N in each functional scenario for analyzing the tooth, distributed in 5 force vectors (18 N each) along the base of the crown, and directed towards its apex. The force vectors were applied in six different angles (15°, 30°, 45°, 60°, and 75°) in relation to the tooth apex, so that angle 0° is completely vertical (Fig. 2A). The functional scenarios tested for the tooth (MPCO.V 0020c) follow the methodology proposed by Torices et al. (2018). The tests simulate the dental serrations in contact with the flesh during bites at different attack angles. The applied force selected do not need to represent the exact bite force of these animals in life to allow comparison of their stress magnitudes and distribution (Jones et al., 2012; Torices et al., 2018). The value applied in our tests is that of a unilateral bite of *Varanus komodoensis* (Moreno et al., 2008), which also corresponds to the estimated maximum bite force of velociraptorines (Therrien, 2005).

For the phalanges, constraints were applied at their base, at the joint surface and flexor tubercles. Forces vectors were applied in three different scenarios to model piercing, scratch-digging, and hook-and-pull. The piercing scenario includes a total force of 400 N applied to the tip of the phalanx, directed against the tip and simulating a puncture function (Fig. 2C, E). The scratch-digging scenario includes one force vector of 400 N at the tip of the ventral surface of the phalanx, simulating the scenario of scraping or cupping (Fig. 2C, E). The hook-and-pull scenario includes three force vectors, 133 N each, at the ventral part of the phalanx, close to its apex, simulating a hook-and-pull function (Fig. 2C, E). The tests on the ungual phalanges (MPCO.V 0022 and MPCO.V 0036a) follow the methodology of Lautenschlager (2014), in which the biomechanical performance of therizinosaur phalanges were tested in simulated scenarios of piercing, hook-and-pull, and scratch-digging. In this methodology, the force used is based on information from the works of Manning (2006; 2009), in which the 400 N were calculated using the approximate weight of *Velociraptor* as a guide.

To solve the models, the scenarios were exported to the software *Abaqus* (v. 6.10; *Simulia*). To access the stress simulated for each model in each scenario, we used von Mises contour plots (Fig. 3) and the von Mises stress was calculated for all elements of each model, creating an average of the stresses of all elements of the 3D model, called the von Mises mean (MVM). To avoid the influence of stress singularities on the von Mises means (MVM), we used an average threshold of 99%. Just like the tooth, our goals with the ungual phalanges are to test how the morphology affects the stress distribution in the different scenarios. As such, it is not

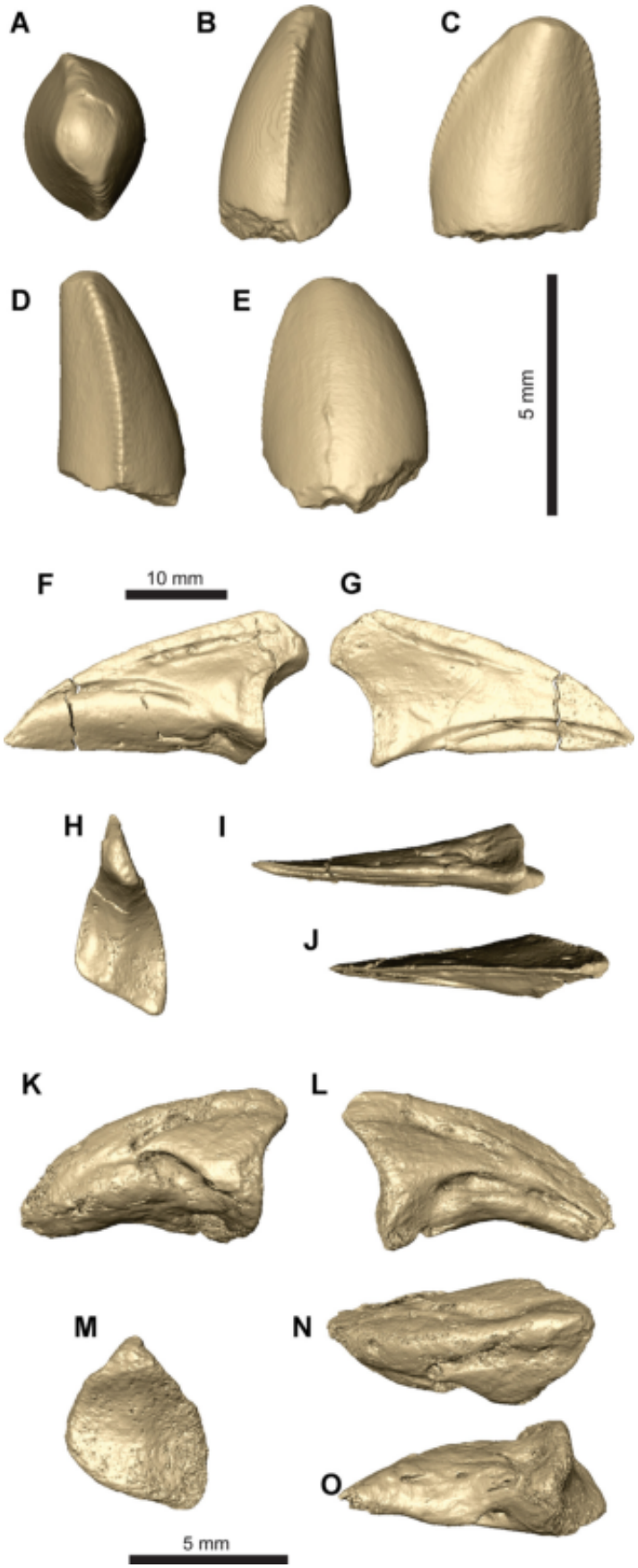

Fig. 1. Isolated tooth and isolated ungual phalanges of *Vespersaurus paranaensis*. (A–E) Isolated tooth MPCO.V 0020c in apical (A), mesial (B), lingual (C), distal (D) and labial (E) views – Scale bar: 5 mm. (F–J) Ungual phalange of a right digit IV MPCO.V 0022 in medial (F), lateral (G), proximal (H), ventral (I) and dorsal (J) views – Scale bar: 10 mm. (K–O) Ungual phalange of a left digit I MPCO.V 0036a in medial (K), lateral (L), proximal (M), dorsal (N) and ventral (O) views - Scale bar: 5 mm.

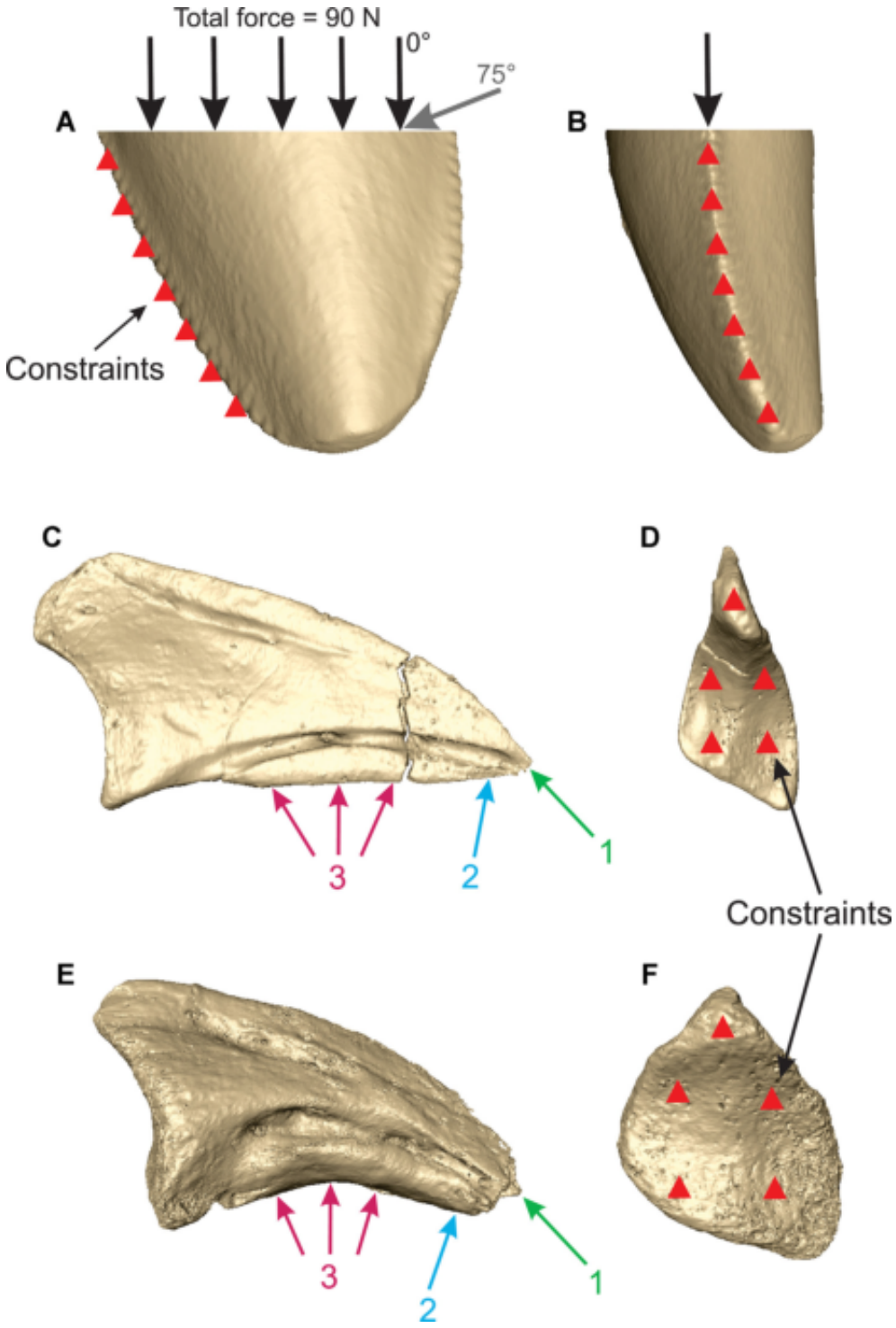

Fig. 2. Loading scenarios of isolated tooth (A–B) and phalanges: right digit IV MPCO.V 0022 (C D) and left digit I MPCO.V 0036a (E–F). The arrows represent the applied forces, and the red triangles represent the location of constraints. In the phalanges: 1 = Piercing; 2 = Scratch Digging; 3 = Hook-and-pull.

necessary that the modeled scenarios include the precise force subject to the ungual phalanges in life, we rather need to standardize the forces applied among materials, the same scale and the same properties, to allow comparisons across taxa and scenarios, as well as results from previous works (Ellis et al., 2008; Dumont et al., 2009). We set the same maximum and minimum limits of the von Mises color scales in all figures in order to stablish a standardized pattern for visualization of the results in FEA analyses.

4. Results

4.1. Tooth

In all tests, the higher stresses are seen on the constrained denticles of the crown (Fig. 3). The 45° angle presented the lowest von Mises stress, with a MVM of 16.61 MPa (Fig. 3), followed by the 60° angle, with MVM = 27.90 MPa (Fig. 3). The test with 0° of

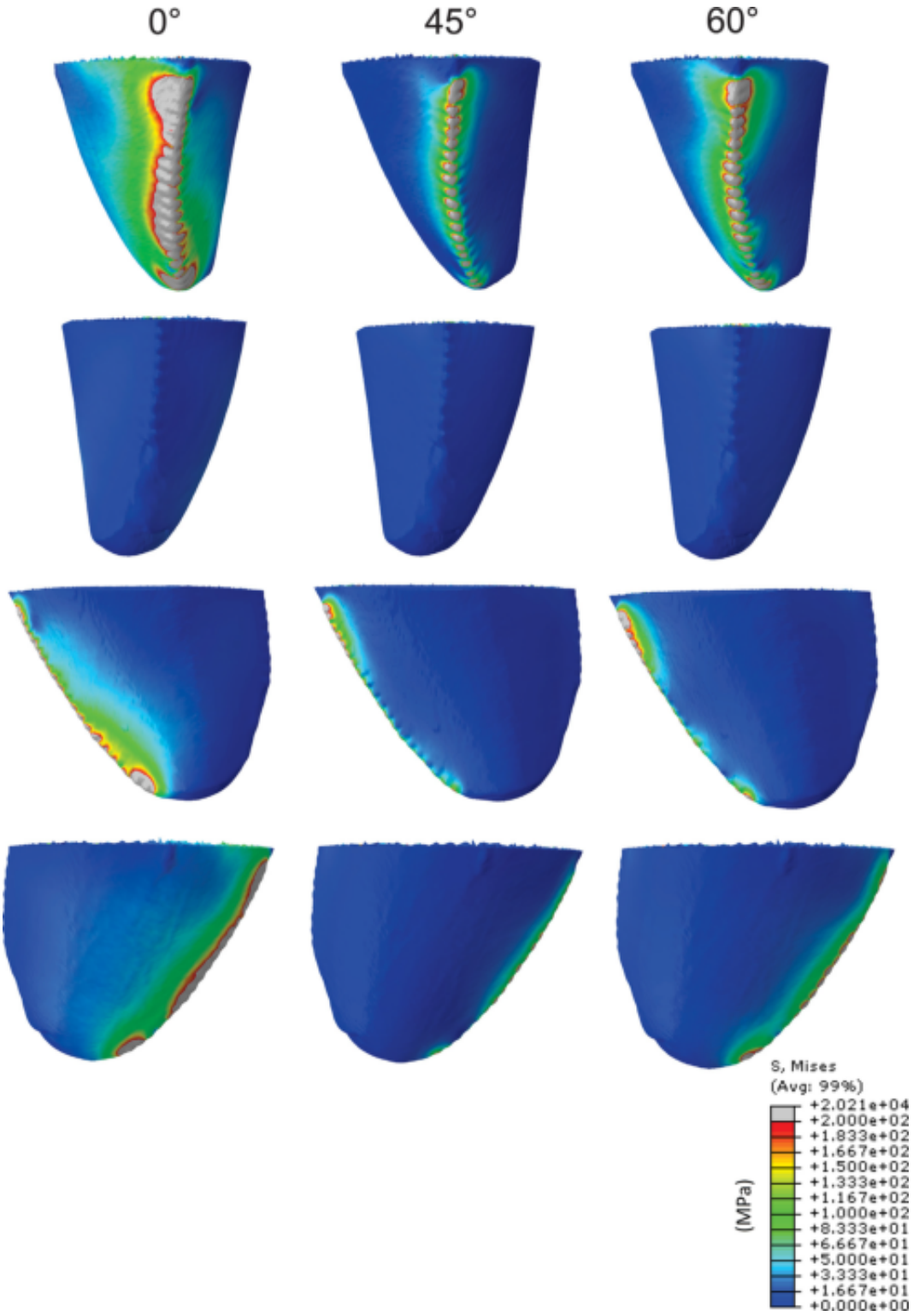

Fig. 3. Von Mises contour plots of *Vespersaurus paranaensis* tooth. In the first column with 0° of inclination, in the second column with 45° of inclination (ideal angle) and the third column with 30° of inclination. The first row is in the distal view, the second row in the mesial view, the third row in the lingual view and the fourth row in the labial view.

inclination presented a greater MVM stress of 52.65 MPa (Fig. 3). The scenarios for 15° and 75° angles show MVM stresses of 33.35 MPa and 33.04 MPa, respectively (see supplemental material for additional figures, von Mises visual plot scale, and the full results of all tests).

4.2. Ungual phalanges

In all scenarios, the phalanges of the right digit IV (MPCO.V 0022) and left digit I (0036a) showed similar patterns of von Mises stress distribution (Fig. 4). In the Piercing scenario, the greatest

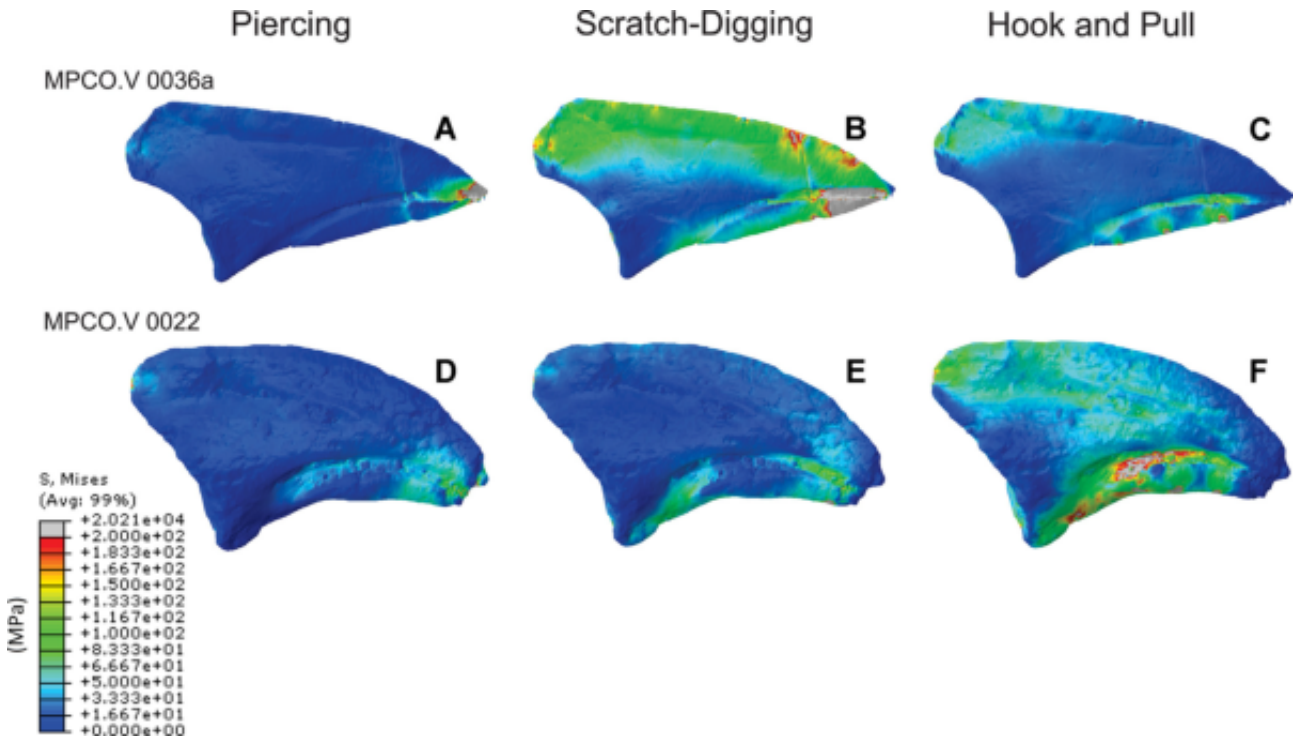

Fig. 4. Von Mises contour plots of ungual phalanges. MPCO.V 0036a in Piercing (A), in Scratch-Digging (B) and in Hook-and-pull (C). MPCO.V 0022 in Piercing (D), in Scratch-Digging (E) and in Hook-and-pull (F).

stress starts at the tip of the element, where the force was applied, also having reduced responses to tension in the tip portion of the base, and in its medial region, with stress distribution inside the groove (Fig. 4A, D). MVM is 0.18 MPa for the left digit I phalanx and 0.11 MPa for the right digit IV phalanx. In the Scratch Digging test, the left digit I phalanx had a higher von Mises stress (MVM = 0.67 MPa) than that of right digit IV (MVM = 0.28 MPa), but the stress distribution patterns were similar, with a greater stress along the dorsal region of the phalanges (Fig. 4B, E). In the Hook-and-pull scenario, the right digit IV phalanx had a lower mean von Mises stress (MVM = 0.18 MPa) than that of left digit I (MVM = 0.26 MPa), but the stress is distributed in about the same areas. A greater stress was detected in the ventral region of the model, where the forces were applied, particularly along the longitudinal grooves (Fig. 4C, F).

5. Discussion

The lowest MVM in the tooth model of *Ves. paranaensis* occurs for the 45° angle scenario. The higher stress levels in our tests with 0°, 15°, 30°, 60°, and 75° angles suggest that the tooth of *Ves. paranaensis* was not adapted to deal with struggling prey, as this would require similar performances in all modeled angles (Torices et al., 2018). In addition, *Ves. paranaensis* is also not adapted for feeding on harder materials, unlike other theropods inferred to have osteophagy (Gignac & Erickson, 2017). Similar results were obtained for troodontid teeth, but not for those of *Dromaeosaurus* and *Saurornitholestes*, which were possibly more adapted to feed on struggling prey (Torices et al., 2018). This is also similar to what is observed in the living lizard *Varanus komodoensis* (Moreno et al., 2008; D'Amore & Blumenschine, 2009) and in the extinct baurusuchid *Aphaurosuchus scharafacies* (Montefeltro et al., 2020; Darlim et al., 2021). An alternative interpretation for the high stress at most tested angles in the *Ves. paranaensis* tooth is that the taxon would prey on animals that did not impose resistance to the teeth, such as smaller vertebrates or softer materials, such as carcasses or invertebrates, not having direct contact with bones or more resistant materials.

Both ungual phalanges (right IV digit and left I digit) showed different stress distribution patterns, some results are similar to those of other theropod phalanges subjected to the same tests (Lautenschlager, 2014). This is the case of the therizinosaurids *Alxasaurus Elesitaiensis* and *Erliansaurus bellamanus*, which have shorter and more robust phalanges, and were interpreted as animals that potentially used the phalanges in a general way, as they performed well in all tested scenarios (Lautenschlager, 2014), as well as the phalange of left digit I. A similar analysis between shape/morphology and von Mises stress distribution are seen in phalanges of mammals with scansorial, fossorial, and terrestrial habits. This is the case of armadillos, which have phalanges capable of performing generalist tasks (Lautenschlager, 2014). The same performance is inferred for the Alvarezsauridae *Mononykus* (Qin et al., 2023), in which the analyzed phalanges do not show greater evidence of specialized functions, presenting similar performances in all tests (Qin et al., 2023). The morphology of the ungual phalanges does not represent the true shape of the phalanges in vivo, as the keratin sheaths that cover them may present another morphology. However, generally for pedal phalanges, keratin sheaths follow the bone morphology in living birds (Hedrick et al., 2019; Thomson & Motani, 2021), but these keratinous structures are very rarely preserved and do not significantly interfere with FEA (Lautenschlager, 2014). Despite the different stress distributions between tests on the phalanges (Fig. 4B, C, E, F), there is no evidence that the phalanges of *Ves. paranaensis* had a specific role because taking all the scenarios into account, there is no specific scenario in which the phalanges performed particularly well when compared to the other scenarios (Fig. 4). Therefore, we suggest that due to the lack of a specific function and its morphology, a generalist use for

the ungual phalanges of *Ves. paranaensis*. Such use is different from that proposed for theropods with slender and long phalanges, such as *Therizinosaurus cheloniformis*, which had specialized phalanges for behaviors that involved less stress on the bones, such as intimidation or sexual display (Nicholls & Russell, 1985; Zanno, 2006; Lautenschlager, 2014; Qin et al., 2023).

6. Conclusion

Finite Element Analysis suggests that the tooth of *Ves. paranaensis* was not adapted for dealing with prey that impose multidirectional loadings, such as those that struggle when captured. It was also not adapted to bite hard materials such as bones, unlike other top predators such as larger theropods and crocodyliforms. The ungual phalanges of *Ves. paranaensis* performed well in the tested FEA scenarios and has similar morphology to other taxa suggested as a generalist, which corroborates a generalist role in the ungual phalanges of *Ves. Paranaensis*. The data obtained via FEA suggest that *Ves. paranaensis* was not a top predator of the Caiuá desert in southeastern Brazil, having a possibly generalist diet, focused on small prey and/or on an opportunistic feeding strategy.

Acknowledgements

This study was partially funded by Coordenação de Aperfeiçoamento de Pessoal de Nível Superior – Brasil (CAPES) – Finance Code 001, for GGB. GGB, FCM, and MCC are funded by FAPESP (process n° 2020/12786-2) and PROBRAL (process n° 88887.628046/2021-00). We thank the City Hall of Cruzeiro do Oeste, Paraná – Brazil, especially the Mayor Maria Helena Bertoco Rodrigues and the Agência Nacional de Mineração (ANM). We thank Cretaceous Research Editor-in-Chief Eduardo Koutsoukos and the two anonymous reviewers that greatly improved this manuscript.

References

Agnolin, F.L., Martinelli, A.G., 2007. Did oviraptorosaurs (Dinosauria; Theropoda) inhabit Argentina? Cretaceous Research 28 (5), 785–790. https://doi.org/10.1016/j.cretres.2006.10.

Batezelli, A., Ladeira, F.S.B., 2016. Stratigraphic framework and evolution of the Cretaceous continental sequences of the Bauru, Sanfranciscana, and Parecis basins, Brazil. Journal of South American Earth Sciences 65, 1–24. https://doi.org/10.1016/j.jsames.2015.11.005.

Bonaparte, J.F., 1996. Cretaceous tetrapods of Argentina. Münchner Geowissenschaftliche Abhandlungen 30, 73–130.

Bonaparte, J.F., Powell, J.E., 1980. A continental assemblage of tetrapods from the Upper Cretaceous beds of El Brete, northwestern Argentina (Sauropoda–Coelurosauria–Carnosauria–Aves). Mémoires de la Société Géologique de France, Nouvelle Série 139, 19–28.

Bright, J.A., 2014. A review of paleontological finite element models and their validity. Journal of Paleontology 88 (4), 760–769. https://doi.org/10.1666/13-090.

Brougham, T., Smith, E.T., Bell, P.R., 2020. Noasaurids are a component of the Australian 'mid'-Cretaceous theropod fauna. Scientific Reports 10, 1428. https://doi.org/10.1038/s41598-020-57667-7.

Bruckmann, M., Hartmann, L.A., Tassinari, C.C.G., Sato, K., Baggio, S.B., 2014. The duration of magmatism in the Serra Geral Group. Parana volcanic province. https://doi.org/10.1016/j.jvolgeores.2017.05.008.

Brum, A.S., Machado, E.B., Campos, D.A., Kellner, A.W.A., 2018. Description of uncommon pneumatic structures of a noasaurid (Theropoda, Dinosauria) cervical vertebra from the Bauru Group (Upper Cretaceous), Brazil. Cretaceous Research 85, 193–206. https://doi.org/10.1016/j.cretres.2017.10.

Carrano, M.T., Sampson, S.D., Forster, C.A., 2002. The osteology of *Masiakasaurus knopfleri*, a small abelisauroid (Dinosauria: Theropoda) from the Late Cretaceous of Madagascar. Journal of Vertebrate Paleontology 22 (3), 510–534. https://doi.org/10.1671/0272-4634(2002)022[0510:TOOMKA]2.0.CO;2.

Carrano, M.T., Loewen, M.A., Sertich, J.J.W., 2011. New materials of *Masiakasaurus knopfleri* Sampson, Carrano and Forster, 2001, and implications for the morphology of the Noasauridae. Smithsonian Contributions to Paleobiology 95, 1–53.

Castro, M.C., Goin, F.J., Ortiz-Jaureguizar, E., Vieytes, E.C., Tsukui, K., Ramezani, J., Batezelli, A., Marsola, J.C.A., Langer, M.C., 2018. A Late Cretaceous mammal from Brazil and the first radioisotopic age for the Bauru Group. Royal Society Open Science 5 (5), 180482. https://doi.org/10.1098/rsos.180482.

Coria, R.A., Salgado, L., 2000. A basal Abelisauria Novas, 1992 (Theropoda-Ceratosauria) from the Cretaceous of Patagonia, Argentina. Gaia 15, 89–102.

D'Amore, D.C., Blumenschine, R.J., 2009. Komodo monitor (*Varanus komodoensis*) feeding behavior and dental function reflected through tooth marks on bone surfaces, and the application to ziphodont paleobiology. Paleobiology 35 (3), 525–552. https://doi.org/10.1666/0094-8373-35.4.525.

Darlim, G., Montefeltro, F.C., Langer, M.C., 2021. 3D skull modeling and description of a new baurusuchid (Crocodyliformes, Mesoeucrocodylia) from the Late Cretaceous (Bauru Basin) of Brazil. Journal of Anatomy 00, 1–41. https://doi.org/10.1111/joa.13442.

Dumont, E.R., Grosse, I., Slate, G.J., 2009. Requirements for comparing the performance of finite element models of biological structures. Journal of Theoretical Biology 256 (1), 96–103. https://doi.org/10.1016/j.jtbi.2008.08.017.

Egli, F.B., Agnolín, F.L., Novas, F., 2016. A new specimen of *Velocisaurus unicus* (Theropoda, Abelisauroidea) from the Paso Córdoba locality (Santonian), Río Negro, Argentina. Journal of Vertebrate Paleontology 36 (4). https://doi.org/10.1080/02724634.2016.1119156.

Ellis, J.L., Thomason, J.J., Kebreab, E., France, J., 2008. Calibration of estimated biting forces in domestic canids: comparison of post-mortem and in vivo measurements. Journal of Anatomy 212 (6), 769–780.

Fernandes, L.A., Ribeiro, C.M.M., 2015. Evolution and palaeoenvironment of the Bauru Basin (upper Cretaceous, Brazil). Journal of South American Earth Sciences 61, 71–90. https://doi.org/10.1016/j.jsames.2014.11.007.

Gignac, P.M., Erickson, G.M., 2017. The Biomechanics Behind Extreme Osteophagy in*Tyrannosaurus r*ex. Scientific Reports 7, 2012. https://doi.org/10.1038/s41598-017-02161-w.

Grine, F.E., Judex, S., Daegling, D.J., Ozcivici, E., Ungar, P.S., Teaford, M.F., Sponheimer, M., Scott, J., Scott, R.S., Walker, A., 2010. Craniofacial biomechanics and functional and dietary inferences in hominin paleontology. Journal of Human Evolution 58 (4), 293–308. https://doi.org/10.1016/j.jhevol.2009.12.001.

Hedrick, B.P., Cordero, S.A., Zanno, L.E., Noto, C., Dodson, P., 2019. Quantifying shape and ecology in avian pedal claws: the relationship between the bony core and keratinous sheath. Ecology and Evolution 9, 11545–11556.

Jones, M.E., O'higgins, P., Fagan, M.J., Evans, S.E., Curtis, N., 2012. Shearing mechanics and the influence of a flexible symphysis during oral food processing in *Sphenodon* (Lepidosauria: Rhynchocephalia). Anatomical Record (Hoboken) 295, 1075–1091.

Langer, M.C., Martins, N.O., Manzig, P.C., Ferreira, G.S., Marsola, J.C.A., Fortes, E., Lima, R., Sant'ana, L.C.F., Vidal, L.S., Lorencato, R.H.S., Ezcurra, M.D., 2019. A new desert-dwelling dinosaur (Theropoda, Noasaurinae) from the Cretaceous of south Brazil. Scientific Reports 9 (1), 9379. https://doi.org/10.1038/s41598-019-45306-9.

Lautenschlager, S., 2014. Morphological and functional diversity in therizinosaur claws and the implications for theropod claw evolution. Proceedings of the Royal Society B 281 (1785), 20140497. https://doi.org/10.1098/rspb.2014.0497.

Manning, P.L., Margetts, L., Johnson, M.R., Withers, P.J., Sellers, W.I., Falkingham, P.L., Mummery, P.M., Barrett, P.M., Raymont, D.R., 2009. Biomechanics of dromaeosaurid dinosaur claws: application of X-ray microtomography, nanoindentation, and finite element analysis. The Anatomical Record 292, 1397–1405. https://doi.org/10.1002/ar.20986.

Manning, P.L., Payne, D., Pennicott, J., Barrett, P., 2006. Dinosaur killer claws or climbing crampons? Royal Society Biology Letters 2, 110–112. https://doi.org/10.1098/rsbl.2005.0395.

Menegazzo, M.C., Catuneanu, O., Chang, H.K., 2016. The South American retroarc foreland system: The development of the Bauru Basin in the back-bulge province. Marine and Petroleum Geology 73, 131–156. https://doi.org/10.1016/j.marpetgeo.2016.02.027.

Montefeltro, F.C., Lautenschlager, S., Godoy, P.L., Ferreira, G.S., Butler, R.J., 2020. A unique predator in a unique ecosystem: modelling the apex predator within a Late Cretaceous crocodyliform-dominated fauna from Brazil. Journal of Anatomy 00, 1–11. https://doi.org/10.1111/joa.13192.

Moreno, K., Wrore, S., Clausen, P., McHenry, C., D'Amore, D.C., Rayfield, E.J., Cunningham, E., 2008. Cranial performance in the Komodo Dragon (*Varanus komodensis*) as revealed by high-resolution 3-D finite element analysis. Journal of Anatomy 212 (6), 736–746. https://doi.org/10.1111/j.1469-7580.2008.00899.x.

Nicholls, E.L., Russell, A.P., 1985. Structure and function of the pectoral girdle and forelimb of *Struthiomimus altus* (Theropoda: Ornithomimidae). Palaeontology 28, 643–677.

Novas, F.E., Agnolin, F.L., Ezcurra, M.D., Porfiri, J., canale, J.I., 2013. Evolution of the carnivorous dinosaurs during the Cretaceous: The evidence from Patagonia. Cretaceous Research 45, 174–215. https://doi.org/10.1016/j.cretres.2013.04.001.

Pol, D., Rauhut, W.M., 2012. A Middle Jurassic abelisaurid from Patagonia and the early diversification of theropod dinosaurs. Proceedings of the Royal Society B 279, 3170–3175. https://doi.org/10.1098/rspb.2012.0660.

Poropat, S.F., Pentland, A.H., Duncan, R.J., Bevitt, J.J., Vickers-Rich, P., Rich, P.T.H., 2020. First elaphrosaurine theropod dinosaur (Ceratosauria: Noasauridae) from Australia — A cervical vertebra from the Early Cretaceous of Victoria. Gondwana Research 84, 284–295. https://doi.org/10.1016/j.gr.2020.03.009. ISSN 1342-937X.

Qin, Z., Liao, C.C., Benton, M.J., Rayfield, E.J., 2023. Functional space analyses reveal the function and evolution of the most bizarre theropod manual unguals. Communications Biology 6, 181. https://doi.org/10.1038/s42003-023-04552-4.

Rayfield, E.J., Milner, A.C., Xuan, V.B., Young, P.G., 2007. Functional Morphology of Spinosaur 'Crocodile-Mimic' Dinosaurs. Journal of Vertebrate Paleontology 27 (4), 892–901. https://doi.org/10.1671/0272-4634(2007)27[892:FMOSCD]2.0.CO;2.

Richmond, B.G., Wright, B.W., Grosse, I., Dechow, P.C., Ross, C.F., Spencer, M.A., Strait, D.S., 2005. Finite element analysis in functional morphology. The Anatomical Record 283A (2). https://doi.org/10.1002/ar.a.20169.

Ross, C.F., 2005. Finite element analysis in vertebrate biomechanics. The Anatomical Record 283A (2). https://doi.org/10.1002/ar.a.20177.

Sampson, S.D., Carrano, M.T., Forster, C.A., 2001. A bizarre predatory dinosaur from the Late Cretaceous of Madagascar. Nature 409, 504–506. https://doi.org/10.1038/35054046.

De Souza, G.A., Soares, M.B., Brum, A.S., Zucolotto, M., Sayão, J.M., Weinschütz, L.C., Kellner, A.W.A., 2020. Osteohistology and growth dynamics of the Brazilian noasaurid *Vespersaurus paranaensis* Langer et al., 2019 (Theropoda: Abelisauridae). Paleontology and Evolutionary Science PeerJ 8, e9771. https://doi.org/10.7717/peerj.9771.

de Souza, G.A., Soares, M.B., Weinschütz, L.C., Wilner, E., Lopes, R.T., Araújo, O.M.O., Kellner, A.W.A., 2021. The first edentulous ceratosaur from South America. Scientific Reports 11, 22281.

Therrien, F., 2005. Feeding behaviour and bite force of sabertoothed predators. Zoological Journal of the Linnean Society 145, 393–426. https://doi.org/10.1111/j.1096-3642.2005.00194.x.

Thomson, T.J., Motani, R., 2021. Functional morphology of vertebrate claws investigated using functionally based categories and multiple morphological metrics. Journal of Morphology 282, 449–471.

Torices, A., Wilkinson, R., Arbour, V.M., Ruiz-Omeñaca, J.I., Currie, P.J., 2018. Puncture-and-Pull Biomechanics in the Teeth of Predatory Coelurosaurian Dinosaurs. Current Biology 28 (9), 1467–1474.

Tortosa, T., Buffetaut, E., Vialle, N., Dutour, Y., Turini, E., Cheylan, G., 2014. A new abelisaurid dinosaur from the Late Cretaceous of southern France: palaeobiogeographical implications. Annales de Palaeontologie 100 (1), 63–86. https://doi.org/10.1016/j.annpal.2013.10.003.

Tseng, Z.J., 2009. Cranial function in a late Miocene Dinocrocuta gigantea (Mammalia: Carnivora) revealed by comparative finite element analysis. Biological Journal of the Linnean Society 96 (1), 51–67. https://doi.org/10.1111/j.1095-8312.2008.01095.x.

Xu, X., et al., 2009. A Jurassic ceratosaur from China helps clarify avian digital homologies. Nature 459, 940–944. https://doi.org/10.1038/nature08124.

Zanno, L.E., 2006. The pectoral girdle and forelimb of the primitive therizinosauroid *Falcarius utahensis* (Theropoda, Maniraptora): Analyzing evolutionary trends within Therizinosauroidea. Journal of Vertebrate Paleontology 26, 636–650.

Appendix A. Supplementary data

Supplementary data to this article can be found online at https://doi.org/10.1016/j.cretres.2023.105594.